Volume 7 | Number 4 | 21 February 2015 | Pages 1223–1636

Analytical Methods

www.rsc.org/methods

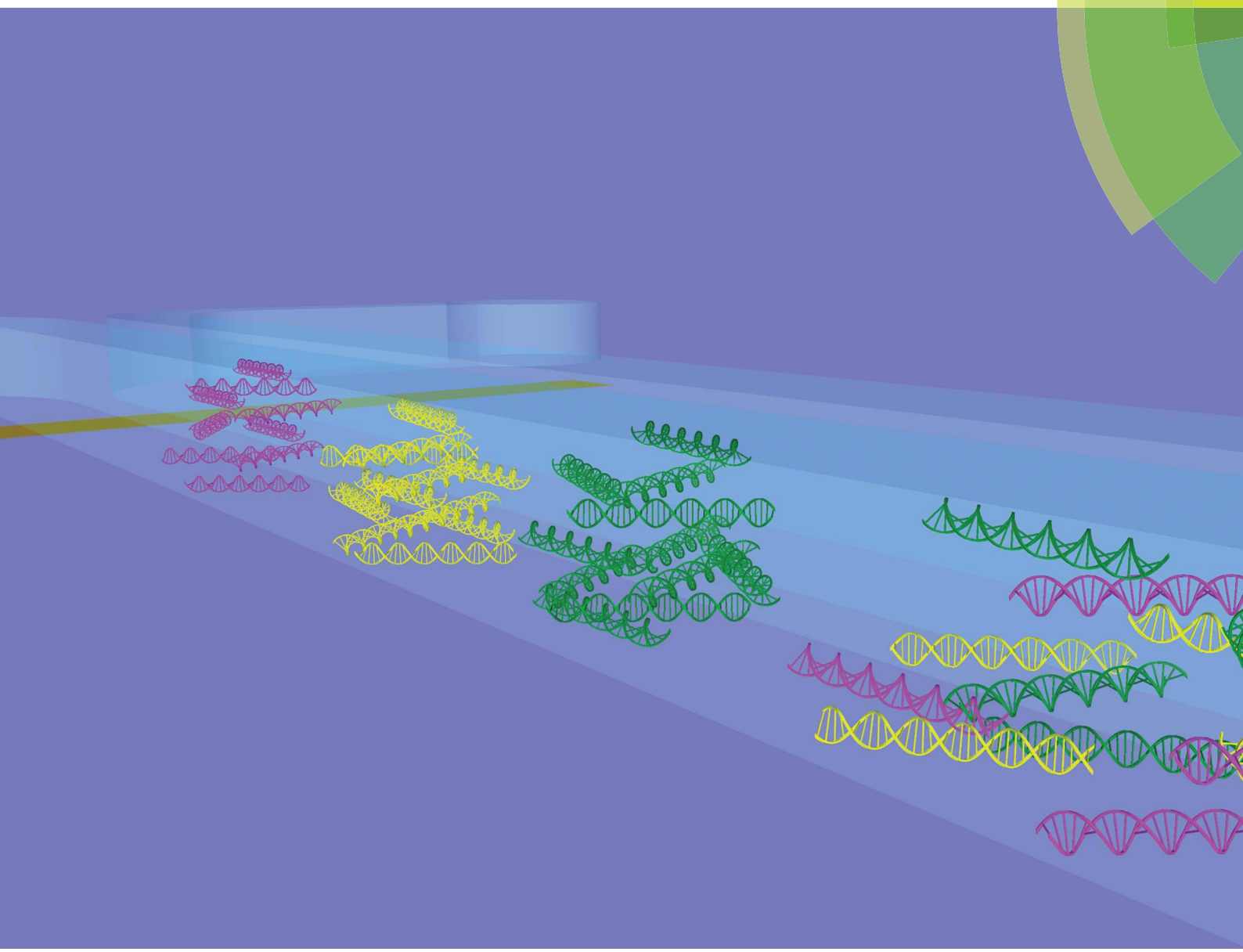

ISSN 1759-9660

ROYAL SOCIETY OF CHEMISTRY

PAPER

Yi Wang *et al.*

Concurrent DNA preconcentration and separation in bipolar electrode-based microfluidic device

Analytical Methods

PAPER

View Article Online
View Journal | View Issue

Cite this: *Anal. Methods*, 2015, **7**, 1273

Concurrent DNA preconcentration and separation in bipolar electrode-based microfluidic device†

Hongjun Song, Yi Wang,* Charles Garson and Kapil Pant

Received 6th August 2014
Accepted 15th October 2014

DOI: 10.1039/c4ay01858c

www.rsc.org/methods

This paper presents a bipolar electrode (BPE) device in a microfluidic dual-channel design for concurrent preconcentration and separation of composite DNA containing samples. The novelty of the present effort relies on the combination of BPE-induced ion concentration polarization (ICP) and end-labeled free-solution electrophoresis (ELFSE). The ion concentration polarization effect arising from the faradaic reaction on the BPE is utilized to exert opposing electrophoretic and electroosmotic forces on the DNA samples. Meanwhile, end-labeled free-solution electrophoresis alters the mass–charge ratio to enable simultaneous DNA separation in free solution. The microfluidic device was fabricated using standard and soft lithography techniques to form gold-on-glass electrode capped with a PDMS microfluidic channel. Experimental testing with various DNA samples was carried out over a range of applied electric field. Concentration ratios up to 285× within 5 minutes for a 102-mer DNA, and concurrent preconcentration and free-solution separation of binary mixture of free and bound 102-mer DNA within 6 minutes was demonstrated. The effect of applied electric field was also interrogated with respect to pertinent performance metrics of preconcentration and separation.

1 Introduction

Microfluidic technology holds great promise for numerous applications in biology, medicine, and chemistry due to their salient advantages, such as low sample volume, fast analysis time, automated processing, and high integrity.[1–3] On-chip analysis[4–6] is one of the key realizations of molecular biology that has been actively studied on integrated microfluidic platforms in the past decade. Despite its merits in integration and automation, traditional microfluidic DNA electrophoresis suffers from several inherent drawbacks, one of which is the need for sieving matrix to overcome the free-draining properties of DNA, leading to prolonged operation, high cost, and low efficiency. To address this issue, end-labeled free-solution electrophoresis (ELFSE) is one of the techniques that has been developed to separate DNA in free solution.[7] In ELFSE, a drag-tag is attached at one end of the DNAs to increase their mass, while keeping the total charge almost unchanged. As a result, the mass–charge ratio of the tag-attached DNA is modified, effecting the separation of unattached and tag-attached DNAs[8] or DNAs of different sizes.[9–12] For example, Ren *et al.* employed ELFSE for the separation and sequencing of single stranded DNA (ssDNA) by using a natural protein, streptavidin, as the drag-tag and the results showed successful sequencing of DNAs.[9] Meagher *et al.* used a genetically engineered protein polymer as the drag-tag to sequence DNA fractions, which demonstrated markedly enhanced resolution than that obtained using natural protein drag-tag.[12] Similar results reported by Won *et al.* have confirmed the feasibility of ELFSE for free solution DNA separation and sequencing up to 233 bases by virtue of engineered protein polymer.[11] Comb-like water soluble copolymers have been synthesized and utilized for ELFSE-based DNA separation, and salient separation of ssDNA up to 150 bases achieved.[10]

Another drawback of the existing microfluidic DNA electrophoresis separation is the low sensitivity due to the trace amount of DNA available for analysis. In addition to nucleic acid amplification, on-chip preconcentration techniques have been developed to tackle this challenge, including field-amplified sample stacking (FASS),[13,14] isoelectric focusing (IEF),[15–17] solid-phase extraction (SPE),[18,19] isotachophoresis (ITP),[20,21] and temperature gradient focusing (TGF).[22,23] FASS relies on the change of electrophoretic velocity near the interface between the low and high concentration buffer. IEF utilizes a pH gradient to focus different molecules according to their isoelectric points. SPE employs an appropriate solid phase to enrich and purify samples through its tunable interactions with biomolecules. ITP concentrates molecular samples in the region between the leading and trailing buffers. TGF generates a temperature gradient, giving rise to an electrophoretic velocity gradient in microchannel to concentrate molecular sample. Despite successful demonstrations, these techniques normally

CFD Research Corporation, Huntsville, AL, USA. E-mail: yxw@cfdrc.com; Fax: +1-256-726-4806; Tel: +1-256-726-4915

† Electronic supplementary information (ESI) available. See DOI: 10.1039/c4ay01858c

entail either complex fabrication or operating protocols or additional immobilized phase.

As an alternative method, ion concentration polarization (ICP) has been extensively investigated and exploited to concentrate various biomolecules. Typically, a micro-nanofluidic junction is utilized to form ICP, which creates an ion depletion layer in front of the junction region due to the extension of the electric double layer (EDL) and the ion-selective nature of the nanostructures.[24] The depletion region then can be utilized to exclude and enrich charged molecules. In general, the micro-nanofluidic junction is constructed by fabricating nanofluidic channel[25,26] or using polymeric nanostructures such as photo-patterned gel[27,28] and ion-selective membrane/polymer[29–34] on a microfluidic platform. Recently, the Crooks group proposed an even simpler preconcentration method termed "faradaic ICP" using bipolar electrode (BPE).[35–45] In contrast to the traditional ICP, this method harnesses faradaic reaction on the surface of the BPE to form an extended, enhanced electric field gradient for biomolecular preconcentration. The homogeneous faradaic reaction adds OH^- and H^+ to the local solution and increases the conductivity close to the poles of the BPE when an external, high electric field is applied across the microchannel. This forms a strong electric field gradient, generating an exclusive depletion zone near the edge of the BPE and exerting exclusive force on ions and molecules.[39] Experimental and numerical investigation demonstrated successful preconcentration of negatively charged fluorescence tracer BODIPY disulfonate in a straight microchannel with a single BPE strip.[35,36] Perdue *et al.* investigated the effect of current and electric field on the concentration enrichment using continuous and discontinuous BPEs. Their results revealed that enrichment occurs at an appreciable faradaic reaction rate, where the faradaic current is coincident with that of concentration enrichment.[38] Laws *et al.* demonstrated simultaneous concentration and separation of three anionic analytes based on their different charges in a PDMS microchannel with a strip of BPE within 200 s.[37] Anand *et al.* measured the evolution of both the electric field gradient and the enriched molecular band in BPE preconcentration, and pointed out that the enrichment is affected by the gradient. More rapid enrichment was achieved at higher buffer concentration and higher electric fields.[40] Sheridan *et al.* presented a method to enrich cationic analyte by coating the microchannel with a positively charged polymer to reverse the direction of electroosmotic flow.[45] Recently Anand *et al.* also reported a new dual-channel configuration to concentrate charged molecules using BPE, which was similar to the traditional ICP except that an electrode strip instead of the micro-nanofluidic junction was employed. Higher enrichment ratio was observed in the dual-channel configuration than by the traditional ICP.[41] Such a dual-channel BPE configuration was further used to separate and enrich both anions and cations by virtue of generating multiple ion depletion zones.[44]

In this paper, we present a simple microfluidic device to concurrently concentrate and separate DNAs by combining dual-channel BPE and end-labeled free-solution electrophoresis (ELFSE). The device relies on the faradaic ICP formed in front of the BPE edge to impose exclusive forces on DNA molecules against carrying electroosmotic flow (EOF) for sample preconcentration. The concurrent DNA separation is enabled by ELFSE, in which a protein drag tag is attached at one end of the DNA to vary its mass–charge ratio. The development represents an original contribution to the microfluidic DNA analysis research that can be used as a simple, generic platform for simultaneous DNA preconcentration and separation for genomic analysis.

2 Methods and materials

2.1 Design and fabrication

The principle and design of the microfluidic BPE device is shown in Fig. 1a. It consists of dual microchannels, in which the top channel is used for loading the buffer solution and the bottom channel for loading the DNA samples. The width of both microchannels is 100 μm and the gap between them is also 100 μm. A single straight electrode with a width of 100 μm located on the floor of the microchannels intersects both microchannels and serves as BPE to provide electric connection between channels. For experimental testing, DNA samples and buffers are loaded from the sample and buffer inlet, respectively. Different voltages are applied at the four reservoirs to generate the electric field. To continuously concentrate and separate DNAs, a high voltage V_1 and a low voltage V_2 are applied at the sample inlet reservoir and outlet reservoir, respectively, with the inlet and outlet reservoirs of the buffer channel grounded ($V_3 = V_4 = 0$). Such an electric setting provides a tangential electroosmotic flow (EOF) moving from right to left (pink arrow) and continuously drives the DNAs from the inlet reservoir towards the intersection between the BPE and the microchannel. Given the voltage drop between the sample

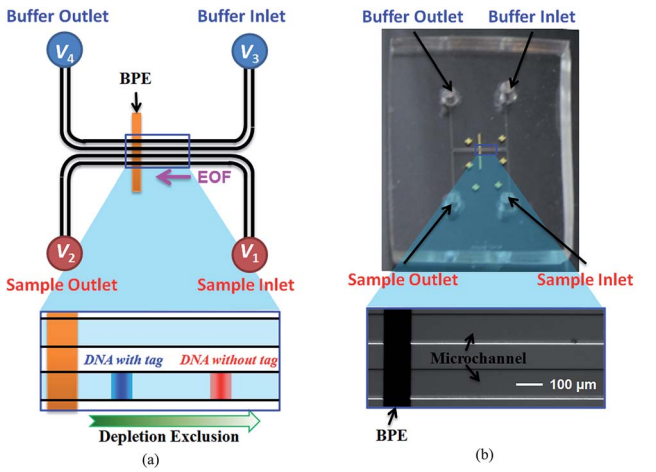

Fig. 1 (a) Schematic of dual-channel microfluidic BPE device. The top channel is used to load the buffer and the bottom channel is used to load the DNA containing samples. A single bipolar electrode (BPE), located at the floor of the channels, intersects both channels; and (b) the assembled device with an enlarged view of the BPE-microchannel junction. The electrode is fabricated using standard lithography with chrome/gold on glass. The fluidic channels are made out of PDMS using soft lithography.

channel and the buffer channel, the faradaic reaction will take place at the surface of the BPE, and an ion depletion zone will form upstream of the BPE to exert an exclusive force on the negatively charged DNAs (from left to the right, as shown in the green arrow in Fig. 1a).[41] As a result, the DNAs will be accumulated and enriched, giving rise to a region with enriched DNAs therein. Meanwhile for molecules with different mass–charge ratios, such as DNAs with or without end-labeled tags, they can be separated along the channel due to the different strengths of the exclusive forces they experience as shown in Fig. 1a, in which the blue and red bands represent the DNAs with or without tags having different mass–charge ratio. Therefore, the concurrent concentration and separation of different DNAs can be achieved.

The device comprises a hybrid PDMS/glass structure and consists of two complimentary layers: (1) a PDMS layer with microfluidic channels; and (2) a BPE fabricated on a glass substrate. The PDMS layer was fabricated using the soft lithography techniques and the patterned gold (with chromium as the adhesion layer) BPE was fabricated using the standard lithography techniques.[46] The height of the microchannel in the PDMS layer is about 5 μm. Both PDMS layer and the glass/BPE substrate were bonded together using O_2 plasma cleaning, followed by heating at 95 °C for 20 minutes on a hot plate. Fig. 1b shows the assembled device with an enlarged view of the BPE-microchannel junction.

2.2 Materials and experimental protocol

A customized 102-mer biotinylated DNA (sequence: 5′-(DyLight547)-AGC AAA ATT TAC CTT GTG TTA CGC TTA GGC AAA TTT ATT TAT TTT TAC TAT GAT CTG GGC GGC GGC AAA CTA GGC CTT GGC CAC GTG AGC GAA AAA GAT GCG-(BioTEG)-3′) labeled with fluorescence DyLight547 was used in the experiments for demonstration. Note that the DNA allows attachment of a streptavidin molecule onto the biotin label at the 3′-end for separation. A mixture of the biotinylated DNA without streptavidin (free DNA) and the DNA with streptavidin bound at its 3′ end (bound DNA) were used for the concurrent preconcentration and separation. These DNA samples were prepared in 5 mM Tris–HCl buffer solution.

The experimental protocol is given as follows: First the fabricated device was treated using 1% BSA for 5 minutes, followed by sequential washing using 100 mM, 10 mM and 5 mM Tris–HCl buffer for 5–10 minutes. Then 5 mM Tris–HCl buffer was loaded into both sample and buffer reservoirs to fill the channels. Finally DNA sample was loaded into the channel through the sample inlet. Meanwhile DC voltages were applied between the reservoirs using a high-voltage power supply (HVS-3000D, Labsmith Corp, Livermore, CA, USA). The preconcentration and separation of DNAs were observed using Nikon TE-2000E epi-fluorescence inverted microscope and the time-lapse images were recorded using a digital camera (CoolSNAP HQ2, Photometrics, Tucson, AZ, USA). Three independent measurements were taken under the same test condition to ensure reproducibility and statistical significance of the experiments.

3 Results and discussion

In this section, DNA preconcentration results will be first presented, followed by the demonstration of the concurrent preconcentration and separation of two DNAs (with or without the streptavidin drag-tag). Finally the effect of the electric field on DNA preconcentration and separation will be discussed using the parametric tests.

3.1 DNA preconcentration

The 102-mer biotinylated DNA without streptavidin (free DNA) with a 50 nM initial concentration was first examined to demonstrate the preconcentration functionality of our device. The voltage difference V_{diff} across the sample channel ($V_{diff} = V_1 - V_2$) was 40 V. Fig. 2a illustrates the fluorescence visualization snapshots at different time points ($t = 0, 1, 2, 3, 4, 5$ min). As can be seen, the DNA gets continuously accumulated and enriched. Further, the exclusion zone indicated by the edge of the DNA band in the sample channel propagated outwards from the BPE due to the dynamic equilibration process of faradaic ICP. The enrichment of DNA and propagation of the exclusion zone was also confirmed by the plot of the fluorescence intensity along the microchannel (as shown in Fig. 2b as well as in Movie_1 in the ESI†). The maximum intensity gradually increased from 0 to 4800 A.U. in 5 minutes. The preconcentration performance of the device was quantitatively characterized by calculating the concentration ratio (defined as the ratio of the enriched concentration, average along the cross-section, to the initial concentration) at different times. As shown in Fig. 2c the concentration ratio increased to 285× within 5 minutes, yielding an average concentration speed of 57× per min.

3.2 Concurrent concentration and separation of DNA mixture

In this section, we present the experimental results of concurrent concentration and separation of the DNA mixture, which consists of the biotinylated DNA without streptavidin (free DNA) and the DNA with streptavidin bound at its 3′-end (bound DNA). The latter was formed by conjugating free DNA to streptavidin. To allow effective conjugation with streptavidin, 100 nM free DNA was incubated with 100 nM streptavidin in equal volume for 30 minutes. The streptavidin attached DNA (bound DNA) was then mixed with free DNA to obtain the mixture sample. The initial concentration of both the bound DNA and the free DNA was 25 nM. To achieve a higher electric field gradient for efficient separation, we increased the voltage difference V_{diff} across the sample channel from 40 V (used in single DNA preconcentration) to 60 V. Fig. 3a illustrates the snapshots at different time points. The movement, concurrent preconcentration and separation of the DNAs in the mixture sample can be clearly observed along with continuously growing separation resolution (see Movie_2 in the ESI†). Note that the free DNA moves faster away from the edge of the BPE, whereas the bound DNA migrates slowly due to the drag imposed by the streptavidin molecule (that counteracts the exclusive force and slows down the movement). Again, the DNA bands propagated

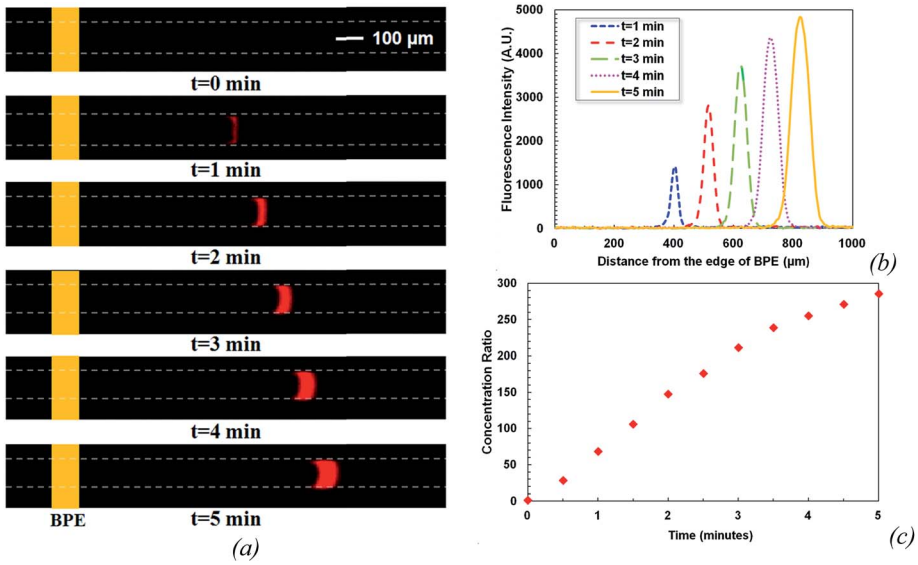

Fig. 2 Preconcentration performance of the dual-channel microfluidic BPE device: (a) fluorescence images at different times points; (b) fluorescence intensity plot along the length of the channel; and (c) concentration ratio *vs.* time.

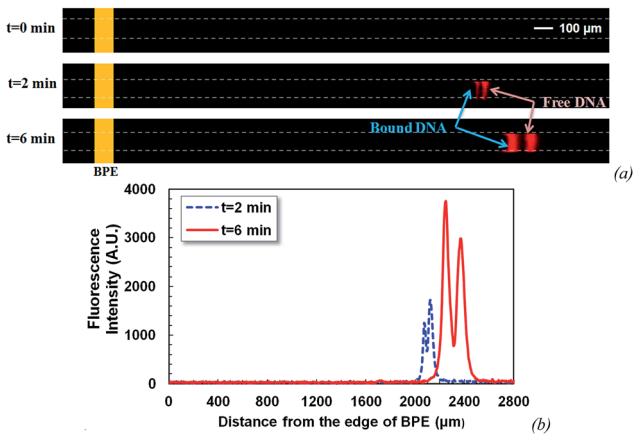

Fig. 3 Concurrent concentration and separation of the free DNA and the bound DNA in the present dual-channel microfluidic BPE device: (a) fluorescence images at different times points; and (b) fluorescence intensity along the channel.

outwards from the edge of the BPE. Note that the movement of the bands may fluctuate due to the dynamic equilibration process of the ICP. In addition to the enrichment of both DNAs, the spacing between the two bands becomes wider as the time elapses, indicating continuously enhanced separation with time. Two saliently resolved DNA bands corresponding to the free DNA and bound DNA were observed at $t = 6$ min (Fig. 3a), confirmed by the fluorescence intensity plot along the channel length as shown in Fig. 3b.

To quantitatively evaluate the device performance, metrics of both the concentration ratio and the separation resolution were calculated from the fluorescence intensity plots. The separation resolution is an important indicator widely used to characterize various separation devices, and is defined as:[47]

$$\mathrm{SR} = \sqrt{2(\ln 2)}\Delta d/(W_{b1} + W_{b2}) \quad (1)$$

where Δd, W_{b1}, and W_{b2} are the distance between the two band peaks, the band width of the bound DNA and the free DNA, respectively, which are calculated as the average values along the channel width. Higher concentration ratio and separation resolution represent better performance. Fig. 4a shows that the concentration ratio for both bound DNA and free DNA increases with the time. The concentration ratio at 6 min approximately reached 600× and 500× for the bound and free DNA, yielding an average concentration speed of 100× per min and 83× per min, respectively. We also hypothesize that the higher concentration ratio and the longer equilibration process of the bound DNA can be potentially attributed to the mass of streptavidin added onto the DNA sample that causes lower diffusivity and lower electrophoretic mobility of the bound DNA in contrast to the free DNA. We noticed that DNA enrichment factor and speed here was larger than that in the previous single DNA preconcentration demonstration due to the usage of a higher voltage difference V_{diff} across the sample channel. Fig. 4b also depicts that the separation resolution also increased from 0.49 to 1.17 as the time elapses, confirming a clear separation between both DNAs after 6 min.

Among all the operating parameters, the difference in the applied electric potential ($V_{diff} = V_1 - V_2$) between the sample inlet and the sample outlet plays the most critical role, and hence, was extensively investigated in the present study. Four different values of the electric potential difference $V_{diff} = 30$ V, 40 V, 60 V and 80 V were investigated. The initial concentration of both the bound and free DNA was roughly set at 25 nM. Fig. 5a illustrates that the concentration ratios of both DNAs grow with the electric field strength, which can be attributed to the stronger exclusive force on them and the faster EOF, both enhancing the concentration performance within a short period

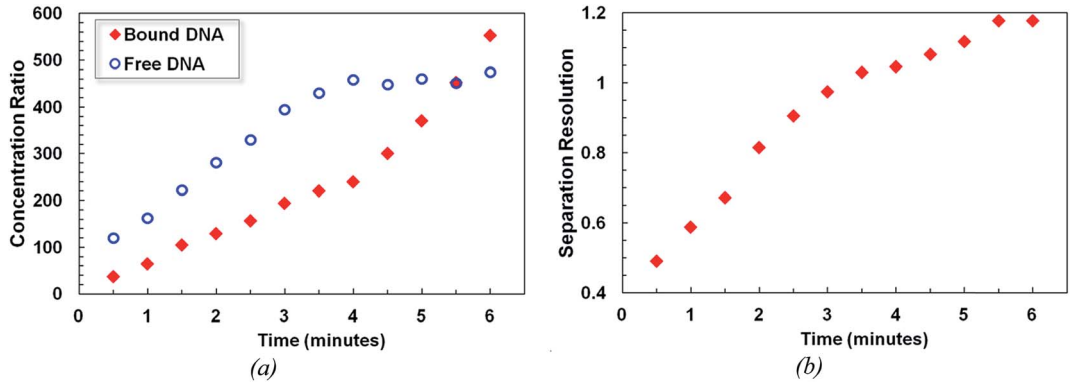

Fig. 4 Quantitative performance analysis of the dual-channel microfluidic BPE: (a) concentration ratio *vs.* time. The concentration speed for bound DNA is lower due to the larger size; and (b) separation resolution *vs.* time.

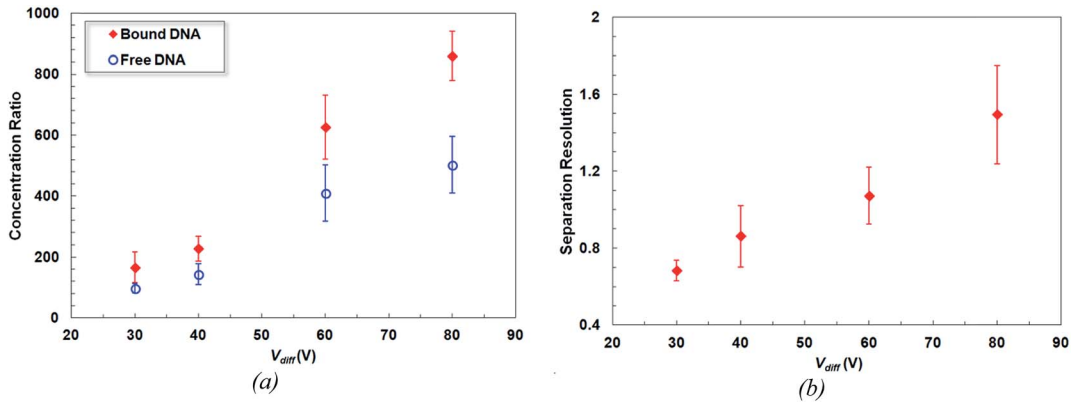

Fig. 5 Effect of the applied electrical potential difference across the sample channel on (a) concentration ratio; and (b) separation resolution.

of time. The final concentration ratio of the bound DNA after 6 min was about 160×, 230×, 630×, 860×, respectively, for V_{diff} = 30 V, 40 V, 60 V and 80 V, corresponding to the average concentration speed of 27× per min, 38× per min, 105× per min and 138× per min. Similarly the final concentration ratio of the free DNA after 6 min was about 100×, 140×, 410×, 500×, corresponding to the average concentration speed of 17× per min, 27× per min, 68× per min and 83× per min, respectively. Fig. 5b shows that the separation resolution also grew from 0.68 to 1.49 as a result of V_{diff} increase from 30 V to 80 V, resulting in enhanced resolution. However, it should be pointed out that there is an upper limit of the applied electric potential to avoid drastic electrolysis near BPE.

4 Conclusion

In this paper we presented a novel microfluidic BPE device for concurrent DNA preconcentration and separation. The device relies on the faradaic ICP phenomenon to harness opposing electrophoretic forces and electroosmotic flow acting on the DNAs at the junction of the microchannel and BPE, as well as the end-labeled free solution electrophoresis to vary the mass–charge ratio for molecular separation. Extensive experiments were carried out to demonstrate the device and quantitatively characterize its performance. Key findings are summarized as below:

(1) The dual-channel microfluidic BPE device effectively concentrated 102-mer biotinylated DNA with 50 nM initial concentration. Concentration ratio of 285× was achieved in 5 min, yielding an average concentration speed of 17× per min.

(2) The concurrent concentration and separation of biotinylated DNAs using streptavidin as the drag tag was successfully accomplished. Concentration ratios of 600× and 500× for bound DNA and free DNA were obtained within 6 min when the potential difference V_{diff} was 60 V, leading to an average concentration speed of 100× per min and 83× per min, respectively.

(3) The investigation on the effect of electric potential indicated that subject to practical constraints (*e.g.*, in particular, electrolysis complication) large electric potential and stronger field allow for higher concentration ratio and separation performance.

Our studies firmly establish the feasibility of the BPE based microfluidic device for concurrent molecule preconcentration and separation, which would significantly contribute the microTAS community, in particular, genomics and proteomics. By carefully engineering drag-tags, desired behavior of ELFSE can be tuned to achieve a practical BPE device for specific

applications. On the other hand our device may also benefit from the development in the area of label free enrichment monitoring[42] and electrochemical gated delivery,[48] among others.

Acknowledgements

This research is sponsored by NIH/NHGRI under grant number 5R44HG004290-03.

References

1 P.-A. Auroux, *et al.*, Micro total analysis systems. 2. Analytical standard operations and applications, *Anal. Chem.*, 2002, **74**(12), 2637–2652.
2 D. R. Reyes, *et al.*, Micro total analysis systems. 1. Introduction, theory, and technology, *Anal. Chem.*, 2002, **74**(12), 2623–2636.
3 G. M. Whitesides, The origins and the future of microfluidics, *Nature*, 2006, **442**(7101), 368–373.
4 G.-B. Lee, *et al.*, Microfabricated plastic chips by hot embossing methods and their applications for DNA separation and detection, *Sens. Actuators, B*, 2001, **75**(1), 142–148.
5 R. Ashton, C. Padala and R. S. Kane, Microfluidic separation of DNA, *Curr. Opin. Biotechnol.*, 2003, **14**(5), 497–504.
6 G. W. Slater, *et al.*, The theory of DNA separation by capillary electrophoresis, *Curr. Opin. Biotechnol.*, 2003, **14**(1), 58–64.
7 R. J. Meagher, *et al.*, End-labeled free-solution electrophoresis of DNA, *Electrophoresis*, 2005, **26**(2), 331–350.
8 P. Mayer, G. W. Slater and G. Drouin, Theory of DNA sequencing using free-solution electrophoresis of protein-DNA complexes, *Anal. Chem.*, 1994, **66**(10), 1777–1780.
9 H. Ren, *et al.*, Separating DNA sequencing fragments without a sieving matrix, *Electrophoresis*, 1999, **20**(12), 2501–2509.
10 R. D. Haynes, *et al.*, Comblike, monodisperse polypeptoid drag-tags for DNA separations by end-labeled free-solution electrophoresis (ELFSE), *Bioconjugate Chem.*, 2005, **16**(4), 929–938.
11 J.-I. Won, R. J. Meagher and A. E. Barron, Protein polymer drag-tags for DNA separations by end-labeled free-solution electrophoresis, *Electrophoresis*, 2005, **26**(11), 2138–2148.
12 R. J. Meagher, *et al.*, Sequencing of DNA by free-solution capillary electrophoresis using a genetically engineered protein polymer drag-tag, *Anal. Chem.*, 2008, **80**(8), 2842–2848.
13 B. Jung, R. Bharadwaj and J. G. Santiago, Thousandfold signal increase using field-amplified sample stacking for on-chip electrophoresis, *Electrophoresis*, 2003, **24**(19–20), 3476–3483.
14 J. Lichtenberg, E. Verpoorte and N. F. de Rooij, Sample preconcentration by field amplification stacking for microchip-based capillary electrophoresis, *Electrophoresis*, 2001, **22**(2), 258–271.
15 D. Kohlheyer, *et al.*, Microfluidic high-resolution free-flow isoelectric focusing, *Anal. Chem.*, 2007, **79**(21), 8190–8198.
16 K. Macounová, C. R. Cabrera and P. Yager, Concentration and separation of proteins in microfluidic channels on the basis of transverse IEF, *Anal. Chem.*, 2001, **73**(7), 1627–1633.
17 J. Wen, *et al.*, Microfluidic preparative free-flow isoelectric focusing: system optimization for protein complex separation, *Anal. Chem.*, 2010, **82**(4), 1253–1260.
18 B. S. Broyles, S. C. Jacobson and J. M. Ramsey, Sample filtration, concentration, and separation integrated on microfluidic devices, *Anal. Chem.*, 2003, **75**(11), 2761–2767.
19 J. P. Kutter, S. C. Jacobson and J. M. Ramsey, Solid phase extraction on microfluidic devices, *J. Microcolumn Sep.*, 2000, **12**(2), 93–97.
20 B. Jung, R. Bharadwaj and J. G. Santiago, On-chip millionfold sample stacking using transient isotachophoresis, *Anal. Chem.*, 2006, **78**(7), 2319–2327.
21 A. Wainright, *et al.*, Sample pre-concentration by isotachophoresis in microfluidic devices, *J. Chromatogr. A*, 2002, **979**(1), 69–80.
22 T. Matsui, *et al.*, Temperature gradient focusing in a PDMS/glass hybrid microfluidic chip, *Electrophoresis*, 2007, **28**(24), 4606–4611.
23 D. Ross and L. E. Locascio, Microfluidic temperature gradient focusing, *Anal. Chem.*, 2002, **74**(11), 2556–2564.
24 A. Plecis, R. B. Schoch and P. Renaud, Ionic transport phenomena in nanofluidics: experimental and theoretical study of the exclusion-enrichment effect on a chip, *Nano Lett.*, 2005, **5**(6), 1147–1155.
25 T. Kim and E. Meyhofer, Nanofluidic concentration of selectively extracted biomolecule analytes by microtubules, *Anal. Chem.*, 2008, **80**(14), 5383–5390.
26 Y.-C. Wang and J. Han, Pre-binding dynamic range and sensitivity enhancement for immuno-sensors using nanofluidic preconcentrator, *Lab Chip*, 2008, **8**(3), 392–394.
27 R. Dhopeshwarkar, L. Sun and R. M. Crooks, Electrokinetic concentration enrichment within a microfluidic device using a hydrogel microplug, *Lab Chip*, 2005, **5**(10), 1148–1154.
28 R. J. Meagher and N. Thaitrong, Microchip electrophoresis of DNA following preconcentration at photopatterned gel membranes, *Electrophoresis*, 2012, **33**(8), 1236–1246.
29 L. F. Cheow, *et al.*, Increasing the sensitivity of enzyme-linked immunosorbent assay using multiplexed electrokinetic concentrator, *Anal. Chem.*, 2010, **82**(8), 3383–3388.
30 H. Chun, T. D. Chung and J. M. Ramsey, High yield sample preconcentration using a highly ion-conductive charge-selective polymer, *Anal. Chem.*, 2010, **82**(14), 6287–6292.
31 J. H. Lee, Y.-A. Song and J. Han, Multiplexed proteomic sample preconcentration device using surface-patterned ion-selective membrane, *Lab Chip*, 2008, **8**(4), 596–601.
32 J. H. Lee, *et al.*, Increase of reaction rate and sensitivity of low-abundance enzyme assay using micro/nanofluidic preconcentration chip, *Anal. Chem.*, 2008, **80**(9), 3198–3204.
33 P. N. Nge, *et al.*, Ion-permeable membrane for on-hip preconcentration and separation of cancer marker proteins, *Electrophoresis*, 2011, **32**(10), 1133–1140.

34 M. Shen, *et al.*, Microfluidic protein preconcentrator using a microchannel-integrated Nafion strip: experiment and modeling, *Anal. Chem.*, 2010, **82**(24), 9989–9997.
35 R. Dhopeshwarkar, *et al.*, Electrokinetics in microfluidic channels containing a floating electrode, *J. Am. Chem. Soc.*, 2008, **130**(32), 10480–10481.
36 D. Hlushkou, *et al.*, Electric field gradient focusing in microchannels with embedded bipolar electrode, *Lab Chip*, 2009, **9**(13), 1903–1913.
37 D. R. Laws, *et al.*, Bipolar electrode focusing: simultaneous concentration enrichment and separation in a microfluidic channel containing a bipolar electrode, *Anal. Chem.*, 2009, **81**(21), 8923–8929.
38 R. K. Perdue, *et al.*, Bipolar electrode focusing: the effect of current and electric field on concentration enrichment, *Anal. Chem.*, 2009, **81**(24), 10149–10155.
39 F. MavreÌ, *et al.*, Bipolar electrodes: a useful tool for concentration, separation, and detection of analytes in microelectrochemical systems, *Anal. Chem.*, 2010, **82**(21), 8766–8774.
40 R. K. Anand, *et al.*, Bipolar electrode focusing: tuning the electric field gradient, *Lab Chip*, 2011, **11**(3), 518–527.
41 R. K. Anand, *et al.*, Bipolar Electrode Focusing: Faradaic Ion Concentration Polarization, *Anal. Chem.*, 2011, **83**(6), 2351–2358.
42 E. Sheridan, *et al.*, Label-Free Electrochemical Monitoring of Concentration Enrichment during Bipolar Electrode Focusing, *Anal. Chem.*, 2011, **83**(17), 6746–6753.
43 E. Sheridan, K. N. Knust and R. M. Crooks, Bipolar electrode depletion: membraneless filtration of charged species using an electrogenerated electric field gradient, *Analyst*, 2011, **136**(20), 4134–4137.
44 K. N. Knust, *et al.*, Dual-channel bipolar electrode focusing: simultaneous separation and enrichment of both anions and cations, *Lab Chip*, 2012, **12**(20), 4107–4114.
45 E. Sheridan, *et al.*, Enrichment of Cations *via* Bipolar Electrode Focusing, *Anal. Chem.*, 2012, **84**(17), 7393–7399.
46 H. Song, *et al.*, Chaotic mixing in microchannels *via* low frequency switching transverse electroosmotic flow generated on integrated microelectrodes, *Lab Chip*, 2010, **10**(6), 734–740.
47 E. Buel, *et al.*, Evaluation of capillary electrophoresis performance through resolution measurements, *J. Forensic Sci.*, 2001, **46**(2), 341–345.
48 K. Scida, E. Sheridan and R. M. Crooks, Electrochemically-gated delivery of analyte bands in microfluidic devices using bipolar electrodes, *Lab Chip*, 2013, **13**(12), 2292–2299.